Atmos. Chem. Phys., 11, 9141–9153, 2011
www.atmos-chem-phys.net/11/9141/2011/
doi:10.5194/acp-11-9141-2011
© Author(s) 2011. CC Attribution 3.0 License.

Atmospheric Chemistry and Physics

Interpreting methane variations in the past two decades using measurements of CH_4 mixing ratio and isotopic composition

G. Monteil[1,2], S. Houweling[2,1], E. J. Dlugockenky[4], G. Maenhout[5], B. H. Vaughn[3], J. W. C. White[3], and T. Rockmann[1]

[1]Institute of Marine and Atmospheric Research Utrecht, Utrecht University, Utrecht, The Netherlands
[2]SRON Netherlands Institute for Space Research, Utrecht, The Netherlands
[3]University of Colorado, Boulder, Colorado, USA
[4]Earth System Research Laboratory, Boulder, Colorado, USA
[5]Joint Research Centre, Ispra, Italy

Received: 1 February 2011 – Published in Atmos. Chem. Phys. Discuss.: 25 February 2011
Revised: 8 August 2011 – Accepted: 24 August 2011 – Published: 6 September 2011

Abstract. The availability δ^{13}C-CH_4 measurements from atmospheric samples has significantly improved in recent years, which allows the construction of time series spanning up to about 2 decades. We have used these measurements to investigate the cause of the methane growth rate decline since 1980, with a special focus on the period 1998–2006 when the methane growth came to a halt. The constraints provided by the CH_4 and δ^{13}C-CH_4 measurements are used to construct hypothetical source and sink scenarios, which are translated into corresponding atmospheric concentrations using the atmospheric transport model TM3 for evaluation against the measurements. The base scenario, composed of anthropogenic emissions according to EDGAR 4.0, constant emissions from natural sources, and a constant atmospheric lifetime, overestimates the observed global growth rates of CH_4 and δ^{13}C-CH_4 by, respectively, 10 ppb yr^{-1} and 0.02 ‰ yr^{-1} after the year 2000. It proves difficult to repair this inconsistency by modifying trends in emissions only, notably because a temporary reduction of isotopically light sources, such as natural wetlands, leads to a further increase of δ^{13}C-CH_4. Furthermore, our results are difficult to reconcile with the estimated increase of 5 Tg CH_4 yr^{-1} in emissions from fossil fuel use in the period 2000–2005. On the other hand, we find that a moderate (less than 5% per decade) increase in the global OH concentration can bring the model in agreement with the measurements for plausible emission scenarios. This study demonstrates the value of global monitoring of methane isotopes, and calls for further investigation into the role OH and anthropogenic emissions to further improve our understanding of methane variations in recent years.

Correspondence to: G. Monteil
(g.monteil@uu.nl)

1 Introduction

Methane is the second most important anthropogenic greenhouse gas in terms of radiative forcing (Denman et al., 2007). Its concentration increased from approximately 700 ppb (nmol/mol) during the pre-industrial period to about 1800 ppb today, with an increase of 1000 ppb during the 20^{th} century (Ferretti et al., 2005).

30 to 40% of methane emissions are from natural origin, of which the largest fraction is from wetlands (100 to 231 Tg CH_4 yr^{-1} (Wuebbles and Hayhoe, 2002; Mikaloff Fletcher et al., 2004a). The other emissions are related to anthropogenic activity: agriculture, fossil fuel combustion, biomass burning and waste treatment. Removal of CH_4 from the atmosphere is primarily due to oxidation by OH, in the troposphere and in the stratosphere, resulting in an atmospheric lifetime of approximately 9 yr (Dentener et al., 2003). A small fraction of the methane is also removed by oxidation in soils, and by reactions with chlorine and O(1D) in the stratosphere.

Following a period of continuous increase, the methane concentration growth-rate progressively started to decline after 1990 (Dlugokencky et al., 1998), leading to a stabilization of methane concentrations between 1999 and 2007. Since 2007, measurements suggest that concentrations started are rising again (Dlugokencky et al., 2003, 2009; Rigby et al., 2008).

Dlugokencky et al. (1998) and Francey et al. (1999) proposed that the observed growth-rate slowdown during the 1990s was due to a stabilization of methane sources and sinks. Later, on the basis of inverse modelling of methane concentration and isotopic ratio for the period from 1984 to 2003, Bousquet et al. (2006) explained the growth-rate slowdown mainly by a decrease of fossil fuel emissions from 1987 to 2000, and after 2000 by a reduction of natural wetlands emissions that would have compensated for increasing anthropogenic emissions. This suggests that the slowdown would only be temporary. Indeed, concentrations started to increase again, but only after 2007: the question remains whether such a compensating mechanism can explain the observed growth-rate between 2003 and 2007.

Other studies suggest that the OH sink could have changed during the last decades (Karlsdóttir and Isaksen, 2000; Dentener et al., 2003; Prinn et al., 2005), and hence could explain part of the slowdown observed in the nineties (Wang et al., 2004; Fiore et al., 2006), while allowing an increase of emissions on this period. However this hypothesis is controversial, since estimates of OH concentrations based on inversion of MCF concentrations suggest rather stable OH levels during this period.

Isotope measurements can provide additional information on the source/sink distribution. Each source emits CH_4 with a process specific range of isotopic ratios. Similarly methane removal induces a change in the isotopic composition of the atmosphere. Thus, the isotopic composition of the atmosphere carries information on the relative importance of these processes. As an example, for $^{13}CH_4$, biogenic sources (such as wetlands, agriculture, waste management) tends to deplete the atmosphere in $^{13}CH_4$ (i.e. diminish the $^{13}C/^{12}C$ ratio in atmospheric methane), while thermogenic (fossil fuel, mud volcanoes) and pyrogenic (biomass burning) emissions, as well as all the methane sinks, induce a $^{13}CH_4$ enrichment of the atmosphere.

Isotopic information has been used in different studies, dealing mostly with long term (centennial) evolution of methane sources (Houweling et al., 2000; Ferretti et al., 2005; Lassey et al., 2007; Neef et al., 2010), or the geographical and seasonal distribution of the methane sources and sinks (Mikaloff Fletcher et al., 2004a,b; Quay et al., 1999; Tyler et al., 2007). A few studies investigated the decadal evolution of methane budget (Francey et al., 1999; Lassey et al., 2000; Braünlich et al., 2001; Bousquet et al., 2006), focusing mainly on the period before 2000.

We use a 3-D atmospheric transport model to simulate the evolution of methane concentrations and $\delta^{13}CH_4$ during the period 1970–2010, assuming different source/sink scenarios. We use CH_4 and δ^{13}C-CH_4 measurements to evaluate the likelihood of those scenarios and we propose several hypothesis to explain the observed growth-rate slowdown.

In Sect. 2 we describe the model setup, including a brief description of the model itself, a presentation of the source and sink scenarios and a description of the way we evaluate the scenarios. In Sect. 3, we present the results of our emissions scenarios and discuss the potential effect of the changes in the most important methane cycle components on the recent trends. Finally we present hypotheses to explain the observed global trends in both the CH_4 and δ^{13}C-CH_4.

2 Method

We performed coupled simulations of the decadal evolution of the atmospheric concentrations of CH_4 and δ^{13}C-CH_4 spanning the period from 1970 to 2010, using the 3-D atmospheric transport model TM3 forced by prescribed methane flux scenarios. Our forward modelling approach allows evaluation of different emission scenarios, regarding their ability to reproduce the CH_4 and δ^{13}C-CH_4 measurements.

First we evaluate how well the current knowledge of the methane cycle allows us to reproduce observed global trends. We build a base scenario on the basis of published source/sink scenarios and isotopic fractionation factors (described in Sect. 2.2). From the differences between the observed and simulated concentrations, we then estimate the changes required to bring the base scenario into agreement with the measurements. Sensitivity simulations are then presented to evaluate whether these changes can explain the mismatch. Finally, the results of the sensitivity simulations are used to construct combined scenarios that reproduce the measurements. A summary of the performed simulations can be found in Table 2.

2.1 Model

We used the offline 3-D chemistry-transport model TM3, described in Heimann and Körner (2003). Transport is driven by 6 hourly meteorological fields from the NCEP reanalysis project (Kalnay et al., 1996). Model simulations were carried out at a resolution of 7.5° in latitude, 10° in longitude and 9 vertical sigma levels from the surface to the top of the atmosphere.

The use of a coarse resolution version of the model is sufficient since methane is a well mixed tracer and since we are mainly interested in multi-year trends on large scales. The coarse resolution allows efficient simulation of a period spanning several decades. Meteorological fields for the year 2000 have been recycled for the whole period. It has been verified that the neglect of interannually varying atmospheric dynamics does not influence our results significantly.

CH_4 and $^{13}CH_4$ concentrations were independently calculated. The advective transport of tracers is calculated using the "slope scheme" of Russel and Lerner (1981). The subgrid scale convective air mass fluxes are evaluated using the cloud scheme of Tiedtke (1989), including entrainment and detrainment in updrafts and downdrafts. Turbulent vertical transport is based on stability-dependent vertical diffusion described in Louis (1979).

Table 1. Sources and sinks of methane for the year 2000, and associated isotopic ratios and fractionation factors as used in the base scenario.

Process	Annual flux ($Tg\,CH_4\,yr^{-1}$)	$\delta^{13}C$-CH_4 (‰)	$\alpha_{^{13}CH_4}$
Natural sources:			
Wetlands	182	−59	
Oceans	28	−59	
Mud volcanoes	15	−40	
Termites	19	−57	
Wild Animals	5	−62	
Total natural source	249	−57.76	
Anthropogenic sources:			
Biomass burning	30	−21.8	
Enteric fermentation and Manure management	102	−62	
Landfills and waste waters treatment	59	−55	
Rice	35	−63	
Coal	26	−35	
Oil and Gas	66	−40	
Residential	10	−38	
Total anthropogenic source	328	−49.87	
Total source	577	−53.27	
Sinks			
Tropospheric OH	−488.9		0.995
Stratospheric OH	−28.8		0.995
Stratospheric $O(^1D)$	−0.75		0.987
Stratospheric Cl	−0.38		0.938
Soils	−37.9		0.978
Total sink	−518.8		0.995

2.2 Base scenario

2.2.1 Sinks

Tropospheric CH_4 oxidation by OH radicals was calculated using OH fields from Houweling et al. (1999), scaled by a factor of 0.92 derived from 1,1,1-trichloroethane (MCF) analysis (M. Krol, personal communications, 2009), leading to a mass weighted global mean OH of 9.9×10^5 molec cm^{-3}. We use the JPL recommended reaction rate $k_{OH+CH_4} = 2.65\times10^{-12}\times e^{-1800/T}$ (Sander et al., 2006). CH_4 oxidation in the stratosphere by OH, Cl and $O(^1D)$ is accounted for using oxidized amounts derived from the Cambridge model of Velders (1995); Law and Pyle (1993), a 2-D model of stratospheric chemistry. The use of oxidized amounts was preferred over turnover times to avoid overestimation of the stratospheric sink due to a generally too low age of stratospheric air in the TM3 model (Jones et al., 2001).

Small differences exist between the reaction rate constants of the different methane isotopologues with OH and other oxidants, as quantified by the fractionation factor α, which is defined for $^{13}CH_4$ as:

$$\alpha_{^{13}C/^{12}C} = \frac{k_{^{13}CH_4}}{k_{^{12}CH_4}} \quad (1)$$

The fractionation factors that were used are listed in Table 1. Values <1 imply that methane removal leads to enrichment of the atmosphere in $^{13}CH_4$.

2.2.2 Sources

Anthropogenic emissions

For the period 1970 to 2005, all anthropogenic emissions except biomass burning are based on the EDGAR4.0 inventory (http://edgar.jrc.ec.europa.eu), which provides yearly maps of emissions on $0.1^\circ\times0.1^\circ$ grid.

Uncertainties associated to these sources are ±39 % for energy use (oil and gas, coal, residential), ±36 % for agricultural emissions (enteric fermentation, manure management, rice) and ±42 % for landfills and waste water treatments emissions (Maenhout, personal communications, 2010).

The period 2006–2010 is not covered by EDGAR4.0. We choose to recycle the emission maps from the year 2005, multiplied by a scaling factor to take into account the evolution of the emissions during this period. Scaling factors were defined as follow: for fossil fuel sources (oil, gas, coal), we derived a scaling factor from BP statistics of fossil fuel production (http://www.bp.com); for all other sources we applied a scaling factor corresponding to a growth rate equivalent to the average 2000–2005 growth rate.

Table 2. Performed sensitivity simulations.

Code	Description
S0	Initial scenario: constant natural sources, and anthropogenic sources growth-rates taken from the EDGAR4.0 inventory, as described in Sect. 2.2.2.
S1	Reduction of wetland emissions by 20 % between 2001 and 2006, 10 % in 2001 and 2007 and 5 % in 2000 and 2008, compared to S1.
S2	Increase of wetland emissions by 1.5 % yr^{-1} after 2000.
S3	Reduction of biomass burning emissions by 5 % in 2000, 10 % in 2001 and 2009, 15 % between 2002 and 2004 and 20 % between 2005 and 2008, compared to S1.
S4	Growth rate of fossil fuel related sources (Coal, oil and gas) of 1 % yr^{-1} after 2000
S5	Increase of OH concentrations by 0.3 % yr^{-1} between 1985 and 1999, and 0.5 % yr^{-1} after 2000.
P1	10 % reduction of wetland emissions between 2002 and 2006, 18 % reduction of biomass burning emissions between 2002 and 2008, 1 % yr^{-1} growth rate of fossil fuel emissions from 2000 to 2005
P2	0.2 % yr^{-1} increase of OH concentrations from 1985 to 2000, 0.6 % yr^{-1} increase of OH after 2000, 18 % decrease of biomass burning emissions between 2002 and 2008, 0.5 % yr^{-1} growth-rate of wetland emissions after 2000.

Biomass burning is the only partly anthropogenic source which is not provided by the EDGAR4.0 inventory. The relative uncertainties associated with it are very large: IPCC 4th assessment report (Denman et al., 2007) lists estimates ranging from 14 Tg CH_4 yr^{-1} (Scheele et al., 2002) to 88 Tg CH_4 yr^{-1} (Mikaloff Fletcher et al., 2004a). This is explained by the high spatial and temporal variability of biomass burning, but also by the difficulty to determine the emission ratios of CH_4, CO and CO_2 emitted by each fire type. We constructed a climatological biomass burning year from the GFEDv2.1 inventory (Randerson et al., 2007), by averaging the emissions over the reported period of 1997–2005, and scaled it up to a value of 30 TgCH_4 yr^{-1}. This approach neglects interannual variability, justified by our focus on longer-term trends, and assumes an insignificant trend of global biomass burning emissions during the target period of our simulations.

Natural sources

The largest uncertainties in the global methane budget come from natural sources, such as natural wetlands and geologic sources. Several studies estimated their strength either by bottom-up or top-down approaches, however, the range of estimates remains very high. Little is known about their long-term trends but they are commonly assumed to be small compared to changes in anthropogenic sources. As a first guess, in the base scenario they are assumed constant.

According to IPCC 4th assessment report (Denman et al., 2007), natural wetland emissions range from 100 Tg CH_4 yr^{-1} (Wuebbles and Hayhoe, 2002) to 231 Tg CH_4 yr^{-1} (Hein et al., 1997; Mikaloff Fletcher et al., 2004a), and only very few studies address the temporal evolution of wetland sources. Walter et al. (2001) and Bousquet et al. (2006) shows no trend respectively during the 1983–1993 and the 1983–2003 periods, while the LPJ-WhyMe model shows a 10 % increase between 1990 and 2005, due to increases in temperature and in vegetation productivity (Wania et al. (2011), and R. Spahni, personal communications, 2010). Because of the large uncertainty of wetland emissions, we use this process to close the global budget of our model simulations. Given the values of all other sources and sinks in the year 1990, 182 Tg CH_4 yr^{-1} are needed to match the observed concentration and mixing ratio (see Sect. 2.2.2). In the absence of clear information about methane trends, we initially assume this value to be constant throughout the whole simulation. In the absence of clear information about trends in wetland emissions, we initially assume year-to-year constant emissions.

Wetland emission fields were constructed by averaging methane fluxes from LPJ-WhyMe for the period 1990–2005 (Wania et al. (2011), and R. Spahni, personal communications, 2010). Based on the work of Sanderson (1996), a value of 20 Tg CH_4 yr^{-1} was used for methane emissions by termites. Geological sources were estimated by Etiope et al. (2008) to be between 30 and 70 Tg CH_4 yr^{-1}, including emissions from terrestrial and oceanic mud volcanoes. We choose intermediate values of 15 Tg CH_4 yr^{-1} for terrestrial mud volcanoes, and 28 Tg CH_4 yr^{-1} for oceanic emissions.

Isotopic values

Emission fields for $^{13}CH_4$ were derived from the CH_4 emission fields by associating each source process with an isotopic source signature δ^{13}C-CH_4, which is assumed constant in time and space, and defined as:

$$\delta^{13}\mathrm{C}-\mathrm{CH}_4 = \left(\frac{\left(^{13}\mathrm{C}/^{12}\mathrm{C}\right)_{\mathrm{src}}}{R_{\mathrm{PDB}}} \right) \quad (2)$$

R_{VPDB} is the isotopic ratio of Vienna Pee-Dee belemnite (de Laeter et al., 2003). The respective source signatures, listed in Table 1, are mostly taken after Houweling et al. (2006). Not all sources have received the same attention in literature, hence it is hard to express uncertainties ranges based solely on the reported ranges. As examples, values of δ^{13}C-CH_4 ranging from −67 ‰ to −53 ‰ have been reported for wetlands (Quay et al., 1988), Yamada et al. (2006)

reported δ^{13}C-CH_4 from biomass burning emissions ranging from −32 ‰ to −16 ‰ and Etiope et al. (2007) reported δ^{13}C-CH_4 from −69 ‰ to −34 ‰ for emissions from mud volcanoes. These ranges reflect mostly the site to site variability of fractionation factors, rather than measurement uncertainty. In many cases they can be explained by site specific conditions (for example C3 versus C4 vegetation in the case of biomass burning). Nevertheless, substantial uncertainty is involved in translating such measurements into the global average fractionation factors used in TM3.

To obtain a budget that satisfies the constraints imposed by the long term mean observed levels of CH_4 and δ^{13}C-CH_4, we adjusted the strength of wetlands and biomass burning sources to the values of respectively 182 and 30 $TgCH_4\,yr^{-1}$. These values are well in the range of fluxes described in the IPCC report (Denman et al., 2007), although on the high-end side for wetlands. Since wetlands and biomass burning are two constant sources in our initial budget, this adjustment has no effect on the CH_4 and δ^{13}C-CH_4 trends, which are our main interest.

2.2.3 Initial conditions

The choice of initial conditions is critical because of the long relaxation times involved in the simulations of CH_4 and δ^{13}C-CH_4. The relaxation time of an atmospheric tracer is the time needed for its concentration to reach a new steady state after a perturbation. In our case the relaxation time is the time during which the simulated concentration is influenced by the chosen initial state.

The relaxation time of one tracer can be approximated by its chemical lifetime In our model, perturbations of CH_4 and ^{13}C-CH_4 decay exponentially with a relaxation time corresponding to the chemical turnover time of approximately nine years. However in the case of δ^{13}C-CH_4 we are dealing with a non-linear relation between two tracers, which results in an extension of the relaxation time (and hence of the length of the required initialization period), as shown by Tans (1997).

For this reason it is not easy to determine the required length of the initialization period.

Theoretically, a simulation reproducing perfectly the state of the atmosphere at the beginning of the simulation would have no influence on the simulation, and all the deviation from the actual state of the atmosphere in the simulation would be the result of errors in the source/sink scenario or in the transport model. We tried to approximate this state by prescribing initial concentrations of CH_4 and $^{13}CH_4$ in agreement with available measurements (Ferretti et al., 2005; MacFarling Meure et al., 2006; Etheridge et al., 1998; Mischler et al., 2009): We initialized our model with hemispherically uniform mixing ratios in 1970. For the Northern Hemisphere we use $CH_4 = 1357$ ppb and δ^{13}C-$CH_4 = -48$ ‰; In the Southern Hemisphere we use $CH_4 = 1343$ ppb and δ^{13}C-$CH_4 = -48.5$ ‰. The intra-hemispheric gradients are

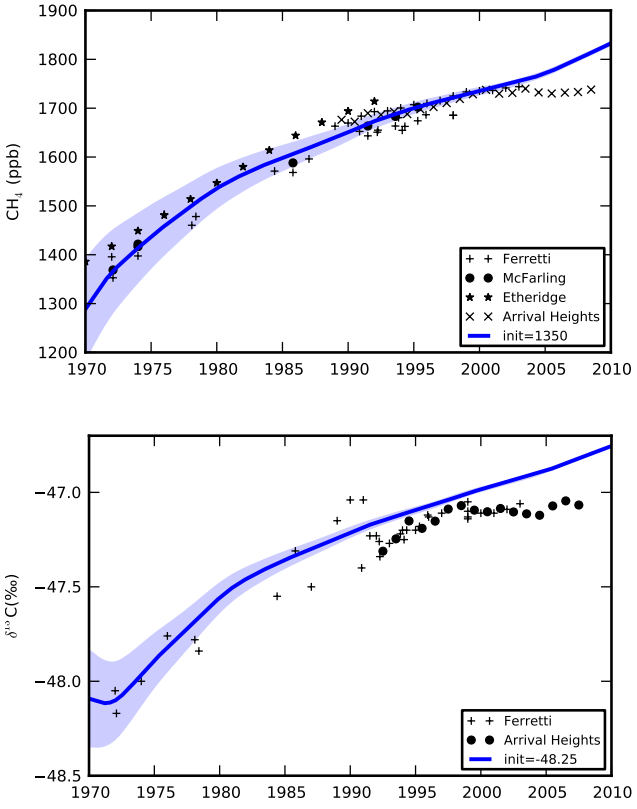

Fig. 1. Comparison between model base scenario and measurements from ice-cores, firn by Etheridge et al. (1998),Ferretti et al. (2005) and MacFarling Meure et al. (2006), and yearly averaged atmospheric measurements at Arrival Heights for CH_4 and δ^{13}C-CH_4. Solid blue line corresponds to simulations using mean initial values of 1350 ppb for CH_4 and −48.25 ‰ for δ^{13}C-CH_4. Shaded areas represent uncertainty ranges of ±100 ppb for methane and ±0.5 ‰ for δ^{13}C-CH_4.

determined by transport, and therefore relax within several months.

To verify our initialization approach we ran several simulations with initial methane mixing ratios ranging from 1250 ppb to 1450 ppb, and δ^{13}C-CH_4 ranging from −48 ‰ to −48.5 ‰. Results are shown in Fig. 1. For initial concentrations or isotopic ratios within the range of uncertainty of the observations, the different simulations converge to less than 10% of their initial difference, which is sufficiently small to not significantly influence the results of our analysis.

2.2.4 Observations

The results of our model simulations were validated using ground-based measurements of CH_4 by NOAA-ESRL (Dlugokencky et al., 2010) and NIWA (Allan et al., 2005). Firn and ice-core measurements were used for the period before 1990 (Ferretti et al., 2005; MacFarling Meure et al., 2006; Etheridge et al., 1998).The measurements were filtered for

non-background conditions, using the information provided in the measurement datasets.

CH_4 isotope measurements are available only for a limited numbers of sites and measurements records span shorter time periods. Since 1999, δ^{13}C-CH_4 is measured at several NOAA sampling sites by University of Colorado – INSTAAR (Miller et al., 2002). The longest time series are available from the NIWA sites Arrival-Heights and Baring-Head, spanning the period from 1991 to 2007 (Allan et al., 2005; Lassey et al., 2010). In addition, measurements from a few other laboratories are available for the 1990s (Quay et al., 1999; Tyler et al., 2007; Bergamaschi et al., 2000; Francey et al., 1999).

For the sites Baring-Head, Barrow, Cape-Grim, Mauna-Loa and Tuilata we built long time-series by combining measurements from Quay et al. (1999) and from the INSTAAR network (Miller et al., 2002). However, the internal consistency of the combined datasets is difficult to verify because of a time gap between them (from 1996 to 1999).

In this paper, we only show results for Barrow (71° N, 159° W), Mauna-Loa (20° N, 156° W), Cape-Grim (41° S, 145° E and Arrival Heights (80° S, 167° E), which are four background stations, providing a good overview of methane and δ^{13}C-CH_4 interannual variability in several latitudinal bands.

2.2.5 Scenario evaluation

A global mass balance inversion has been used to assist the interpretation of the differences between measured and model simulated concentrations in terms of corresponding CH_4 sources and sinks. Each year t, the change in the global atmospheric burden of CH_4 can be written as:

$$\frac{d\mathrm{CH_4}}{dt} = P(t) - L(t) \tag{3}$$

where $CH_4(t)$ is the global atmospheric methane burden, $P(t)$ represents the emissions, and $L(t)$ is a loss term (methane sinks). Neither $P(t)$ nor $L(t)$ are measurable quantities, however $CH_4(t)$, and hence $\frac{d\mathrm{CH_4}}{dt}$, can be inferred from the measurements:

$$\mathrm{CH_4}(t) = H(t) X_{\mathrm{CH_4}}(t) \tag{4}$$

in which $X_{\mathrm{CH_4}}(t)$ is an average measured CH_4 mixing ratio at the surface, and $H(t)$ is a proportionality coefficient translating the average surface mixing ratio into the global atmospheric CH_4 burden.

As methane is a well mixed gas in the troposphere, and as background measurements represent large volumes of air, there is a good correlation between the global burden of methane and the average observed surface concentrations. Therefore it is reasonable to assume that $H(t)$ is a constant.

We determined H by applying Eq. (4) to the year 1990. This year was chosen because good agreement was obtained between the base scenario and the measurements (see Sect. 3).

Equation (3) can then be rewritten as:

$$\frac{d\mathrm{CH_4}}{dt} = H \frac{dX_{\mathrm{CH_4}}(t)}{dt} = P(t) - L(t) \tag{5}$$

The yearly flux correction $\Delta F(t)$ to make our budget consistent with the observations is then:

$$\Delta F(T) = H \frac{dX_{\mathrm{CH_4}}(t)}{dt} - (P_{\mathrm{model}}(t) - L_{\mathrm{model}}(t)) \tag{6}$$

3 Results and discussions

3.1 Base scenario

We first analyse the results obtained with our base scenario S0, described in Sects. 2.2.1 and 2.2.2. Figure 2 compares measurements and model results for CH_4 and δ^{13}C-CH_4 at four different sampling sites (Barrow, Mauna-Loa, Cape-Grim and Arrival Heights), representative of four different latitude bands.

The observed growth rate is close to $10\,\mathrm{ppb\,yr^{-1}}$ before 1990, and progressively declines towards insignificantly low values after 2000. After 2006 the methane concentration started increasing again.

The growth-rate in the period 1985–1995 is reasonably well reproduced by the model: before 1990 the simulated growth rate compares well with the observations, although the model underestimates the observed growth-rate decline after 1990.

Although the observed global growth-rate is best reproduced in the first part of the simulation (1985–1995), the RMS difference between model and observations in the Southern Hemisphere is actually slightly lower between 1990 and 2000. This is explained by the general tendency of the model to overestimate the inter-hemispheric gradient of CH_4. This overestimate has already been reported by Dlugokencky et al. (2003), for the same model, and manifests itself as a time invariant bias, because it does not affect the simulated trend and is therefore not relevant for our analysis.

The δ^{13}C-CH_4 measurements show an increasing trend until 2000, which is quite well reproduced by the model. However, after 2000 the measurements show a stabilization of δ^{13}C-CH_4, while in the model the upward trend continues.

The flux change $\Delta F(t)$ necessary to restore agreement with the measurements was calculated using the procedure described in Sect. 2.2.5. During the period 1990–2000 $\Delta F(t)$ is on average $-6\,\mathrm{Tg\,CH_4\,yr^{-1}}$, with a standard deviation of $15.5\,\mathrm{Tg\,CH_4\,yr^{-1}}$. However, after 2000 $\Delta F(t)$ starts to decrease rapidly, reaching a minimum value of $-40\,\mathrm{Tg\,CH_4\,yr^{-1-1}}$ in 2005. The mean value for the period 2000–2008 is $-25.9\,\mathrm{Tg\,CH_4\,yr^{-1-1}}$, with a standard deviation of $9.4\,\mathrm{TgCH_4\,yr^{-1}}$: a decrease in sources or an increase of the sinks of this order of magnitude is needed to bring the model into agreement with the measurements.

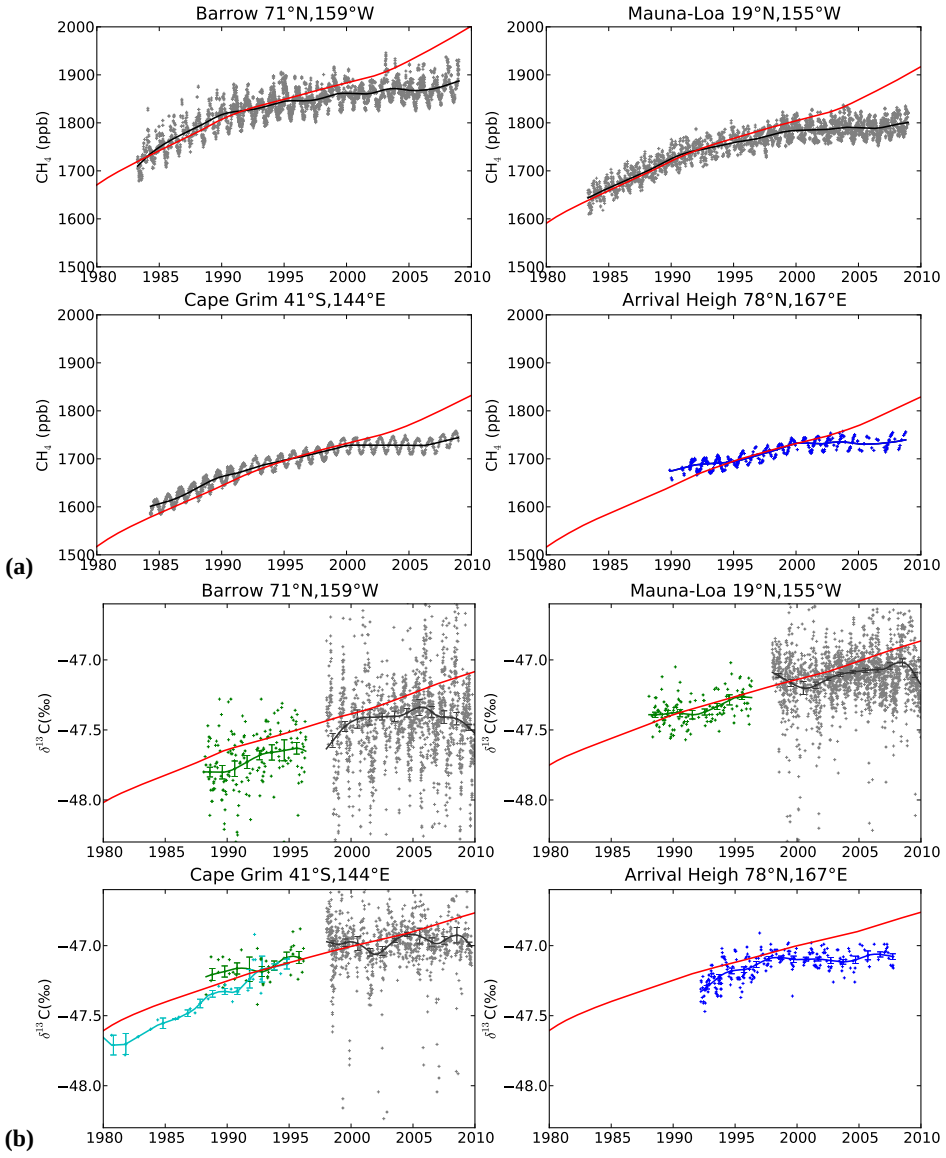

Fig. 2. Comparison between model scenario S0 and measurements for four representative stations, for CH_4 **(a)** and δ^{13}C-CH_4 **(b)**. Model results, shown as solid red lines, are deseasonalized. Measurements, shown as dots (real measurements) and as solid lines (deseasonalized trends), are from: grey: Dlugokencky et al. (2010) (NOAA); light blue: Francey et al. (1999); green: Quay et al. (1999); blue: Allan et al. (2005) (NIWA). Error bars in the trends lines for isotopes represents the yearly uncertainty of the trend.

We have investigated which processes could have been over or underestimated in the period 2000–2006. Anthropogenic emissions may seem a likely candidate since they are the main drivers of the concentration increase in the model. However, reproducing the observed concentrations only by a change in anthropogenic emissions would require a net decrease of those emissions after 2000. Uncertainties of the anthropogenic emissions growth-rate in the EDGAR4.0 inventory for the period 2000–2005 are ±68 % for energy use (oil and gas, coal and residential emissions in Table 1), ±52 % for agriculture (rice, Enteric fermentation and Manure management in Table 1) and ±75 % for landfills and waste water treatment. A lower increase is possible, but a reversal of the trend in this period seems highly unlikely.

Alternatively, a change in another process may have compensated for increased anthropogenic emissions. Since we are dealing with a substantial mismatch, the most likely candidates are the large terms in the CH_4 budget, such as natural wetland emissions and oxidation by OH, or a combination of more than one process.

An important additional constraint is the isotopic ratio. After 2000, atmospheric δ^{13}C-CH_4 remains approximately

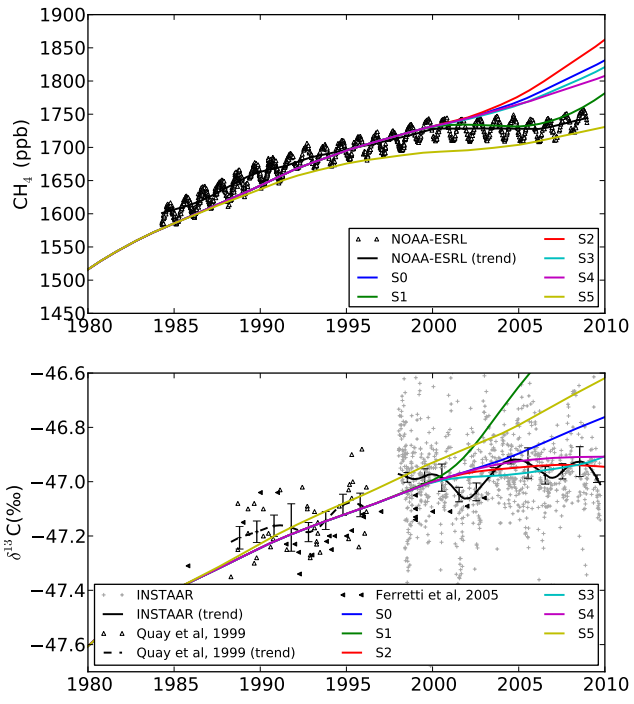

Fig. 3. Comparison between model results for the scenarios S0 to S5 and measurements at the station of Cape-Grim, Australia, for methane (top) and δ^{13}C-CH$_4$ (bottom). Model results are shown as deseasonalized trends (2-yr smoothing). Error bars represent the uncertainty of the calculated trend (yearly RMSE divided by the number of measurements).

in steady state, whereas in the model it increases by 0.3 ‰ yr^{-1} due to the rapid increase of fossil fuel emissions during this period.

In the following we make several sensitivity test simulations to analyse and compare the influence of each process on both CH$_4$ and ^{13}CH$_4$.

3.2 Sensitivity tests

Figure 3 presents the result of the CH$_4$ and δ^{13}C-CH$_4$ sensitivity simulations, which are described in further detail in this subsection and summarized in Table 2. We investigate in detail the three main sources (wetlands; the most heavily enriched source: biomass burning and fossil fuel exploitation), and the main sink process.

3.2.1 Influence of wetlands

Scenario S1 is used to investigate the possibility that increasing anthropogenic emissions have been compensated by a decrease of natural wetland emissions. Conversely, scenario S2 was designed to check whether an increase of wetland emissions could explain the observed discrepancy between modelled and simulated δ^{13}C-CH$_4$. The scenarios are defined as follows:

- S1: emissions from natural wetlands are reduced by 5 % in 2000 and 2008, 10 % in 2001 and 2007 and 20 % between 2002 and 2006 compared to the base scenario (S0). This corresponds to an average reduction of 36.2 Tg CH$_4$ yr^{-1}.
- S2: natural wetland emissions increase by 1.5 % yr^{-1} between 2000 and 2005 and are kept at a the 2005 level after 2006. This corresponds to a total increase of 150 Tg CH$_4$ in 11 yr compared to scenario S0, close to the increase found by the LPJ-Whyme model (Wania et al., 2011).

As can be seen in Fig. 3, scenario S1 brings the simulated CH$_4$ mole fractions into close agreement with the measurements. However, it also leads to an accelerated increase of δ^{13}C-CH$_4$, which further deteriorates the agreement with δ^{13}C-CH$_4$ measurements. This is explained by the fact that a reduction in ^{13}C-CH$_4$ depleted wetland emissions leads to an enrichment of δ^{13}C-CH$_4$ in the atmosphere. Therefore, this scenario could only work if the decrease in wetlands is balanced by strong changes in other fluxes to compensate for the ^{13}C-CH$_4$ enrichment.

Scenario S2 leads to a significantly improved δ^{13}C-CH$_4$ trend compared with S0. It also induces a moderate acceleration of the CH$_4$ growth rate, with a final methane mixing ratio 30 ppb higher than in S0: a moderate increase of wetland emissions to explain the stabilization of the δ^{13}C-CH$_4$ mixing ratio after 2000 is not impossible, however it calls for additional changes that compensate for the extra CH$_4$ emissions and which do not significantly influence the isotopic budget.

3.2.2 Influence of biomass burning

Next we investigate the sensitivity of our model to a temporary change in biomass burning. Global emissions from biomass burning are relatively small compared with emissions from natural wetlands. Therefore, a few percent adjustment of this source is expected to have only a minor impact on the model simulated global trend of CH$_4$.

On the other hand, methane from biomass burning is strongly enriched in ^{13}C (see Table 1) compared to all other methane sources. Therefore δ^{13}C-CH$_4$ is highly sensitive to the biomass burning emissions.

Several sensitivity simulations were carried out to evaluate the possibility that changes in biomass burning influenced the δ^{13}C-CH$_4$ slope after 2006. Simulation S3, presented in Fig. 3 assumes a 1.5% yr^{-1} decrease of biomass burning emissions between 1995 and 2008. This scenario accounts for most of the overestimated δ^{13}C enrichment in the model after 2000, without a significant impact on the CH$_4$ growth rate.

3.2.3 Influence of fossil fuel sources

Detailed analysis of the anthropogenic emissions in EDGAR4.0 points to increasing emissions of fossil fuel derived methane as the main factors explaining the estimated acceleration of methane emissions after 2000. Compared to the average source signature, fossil fuel emissions are enriched in $^{13}CH_4$. Therefore a slower increase of fossil fuel sources could in theory explain part of the discrepancy between modelled and observed CH_4 and $^{13}CH_4$.

In our initial scenario, fossil fuel sources add up to 95 Tg CH_4 in 2000, with an average growth rate of 5 Tg CH_4 yr^{-1} during the period 2000–2010. Attributing the full discrepancy between model and observations to overestimated fossil fuel sources would not be realistic as it would require a strong decrease of these emissions, as shown in Sect. 2.2.5.

We performed a set of sensitivity simulations with growth rates of fossil fuel sources ranging from 0 to 3 % yr^{-1} between 2000 and 2010. For comparison, the growth rate of the base scenario during this period is close to 3 % yr^{-1}.

As shown on Fig. 3, a growth rate of fossil fuel emissions as low as 1 % yr^{-1} would be necessary to explain the δ^{13}C-CH_4 evolution, but this growth-rate reduction is still not large enough to bring the model in agreement with the CH_4 measurements.

It is concluded that an overestimated growth rate of fossil fuel emissions could have contributed to the mismatch between the modelled and observed trends, in particular that of δ^{13}C-CH_4, but cannot be the main factor explaining the CH_4 trend.

3.2.4 Influence of the OH sink

Finally we investigate the potentially important contribution of a trend in methane oxidation by hydroxyl radical. Several studies address the recent evolution of global OH (Prinn et al., 1992; Karlsdóttir and Isaksen, 2000; Lelieveld et al., 2002; Krol and Lelieveld, 2003; Dentener et al., 2003; Prinn et al., 2005, M. van Weele, personal communications, 2010). Generally, these studies fall into two categories: (1) determination of the tropospheric OH burden by inverse modelling of MCF concentrations (2) forward modelling using sophisticated atmospheric chemistry and transport models (ACTM-s). The first approach doesn't provide any significant evidence of a long-term trend. On the interannual time-scale, however, variations of the order of ± 3 % yr^{-1} are predicted (M. van Weele, personal communications, 2010). The second approach predicts an increasing trend of 0.3 to 0.5% yr^{-1} after 1980, which could be attributed to increasing NO_x emissions in the developing countries of the tropics Karlsdóttir and Isaksen (2000).

Our scenario S5 is based on a 0.3% yr^{-1} increase of OH concentrations between 1985 and 2000, and 0.5 % yr^{-1} after 2000, as suggested by Karlsdóttir and Isaksen (2000). Although the OH concentration in S5 starts to differ from S0 from 1985 onwards, the difference between the simulations remains insignificant until 1990, when the difference in OH concentration exceeds 2.5 %. After 1990 the progressive increase in OH leads to a reduction of CH_4 concentrations by 50 to 90 ppb in 2010, compared to S0. The trend in δ^{13}C-CH_4 remains very close to S0 (46.78 ‰ for S5 and 46.88 ‰ for S0, in 2005), consistent with the small fractionation factor of OH oxidation (see Table 1).

This simulation shows that a moderate increase in OH concentrations could account for most of the discrepancy between the observed methane concentrations and the base scenario. However, additional changes in other processes must be involved to explain δ^{13}C-CH_4 measurements.

In these simulations, by recycling the meteorological fields of 2000 we neglect the the influence of temperature trends on the OH+CH_4 reaction rate: Given the JPL recommended rate of $k_{OH+CH_4} = 2.65 \times 10^{-12} \times e^{-1800/T}$ (Sander et al., 2006), the observed temperature increase of 0.2°C between the 1990–1999 and the 2000–2009 period (http://data.giss.nasa.gov/gistemp/graphs/) should lead to a 0.4 % increase in the OH sink, unlikely to significantly affect our results.

3.2.5 Sensitivity to other processes

Besides the processes considered so far, Several other might contribute also to the mismatch between modelled and observed CH_4 and δ^{13}C-CH_4.

For example there is a high uncertainty associated with geological sources (Mud volcanoes, oceans), concerning its global source strength (the estimates vary from 6.6 Tg CH_4 yr^{-1} (Judd et al., 2002) to 45 Tg CH_4 yr^{-1} (Etiope and Milkov, 2004), and its isotopic ratio (measurements range from -33.98 ‰ to -69.43 ‰, Etiope et al., 2007). However, there is no indication for trends in these emissions on the time scale of our simulation, which is short from the perspective of geologic processes. Errors in the size or the isotopic signature of this source in our base scenario would systematically offset the simulated level of CH_4 and δ^{13}C-CH_4, without affecting the simulated trend.

We did not investigate the sensitivity of our simulations to changes in emissions from ruminants or landfills. Since the isotopic signatures of these sources are very similar to wetlands, the sensitivities are also similar. As for wetlands, a decrease in the emissions from ruminants and landfills after 2000 cannot provide an explanation for the observed trends in CH_4 and δ^{13}C-CH_4, since it would lead to further enrichment of the atmosphere in $^{13}CH_4$. However, we cannot exclude a contribution of these processes in combination with other changes.

Allan et al. (2001) suggested a possibly important role of an additional methane sink due to reaction with chlorine radicals in the marine boundary layer. This sink was further investigated in subsequent papers from this

group (Allan et al., 2005, 2007; Lassey et al., 2010), but has not been included in most global studies of the tropospheric methane budget. Although the importance of such a sink would be very minor in terms of methane removal rate, it could potentially have a large impact on the isotope budget because of the strong isotopic fractionation in the reaction Cl+CH_4 (see Table 1).If this chlorine sink has significant interannual variability, as suggested by Allan et al. (2005), then it would strongly affect the δ^{13}C-CH_4 growth-rate and compensating changes in other process would be required to accommodate it in our sources/sinks scenarios. Initial (unpublished) model runs showed that if the trend in Cl were as large as suggested by Allan et al. (2005, 2007), the resulting isotope effects would be unrealistically large. Thus, in the absence of a reliable quantification of a temporal trend in this additional sink term, it was decided not to include it in our study . It should be noted that a temporally constant Cl sink can easily be accounted for: it would simply increase the isotopic fractionation by the total average sink and a more depleted source budget would be needed to fit the observations. However the temporal trends, and hence our conclusions of the present study, would remain the same.

Finally, a known source of error is the treatment of the soil and stratospheric sinks in the model, which are assumed to be the same every year. In reality, however, their sink strengths depend on the atmospheric CH_4 concentration. However, for the studied period the atmospheric burden of methane has changed by less than 10%. Given the fact that these sinks sum up to only 67 Tg CH_4 yr^{-1} in our base scenario, a change smaller than 10 % has a negligible impact.

3.3 Discussion

Results from our base and sensitivity scenarios suggest that the observed slowdown in the growth rate of methane necessarily involves either a decrease of wetland emissions or an increase of methane oxidation by OH, as demonstrated by scenarios S1 and S5.

Other changes cannot be excluded but a realistic deviation from our initial scenario in any other process would have only a minor effect on CH_4, as seen for example in scenarios S3 and S4. It is also very unlikely that the trend of all anthropogenic sources suddenly changed around 2000. Consequently their contribution to the CH_4 growth-rate slowdown can only be secondary.

On the other hand, neither scenario S1 nor scenario S5 satisfy the constraints imposed by δ^{13}C-CH_4 measurements. Additional changes are required to stabilize the δ^{13}C-CH_4 ratio after 2000. We can distinguish two categories of scenarios: with and without changes in OH.

If we assume no trend in OH, the CH_4 growth-rate slowdown can only be explained by decreasing wetland emissions in combination with a decrease in ^{13}C enriched sources (e.g. biomass burning, fossil fuel and maybe mud volcanoes) in a way that balances their counteracting influences on δ^{13}C-CH_4 as observed.

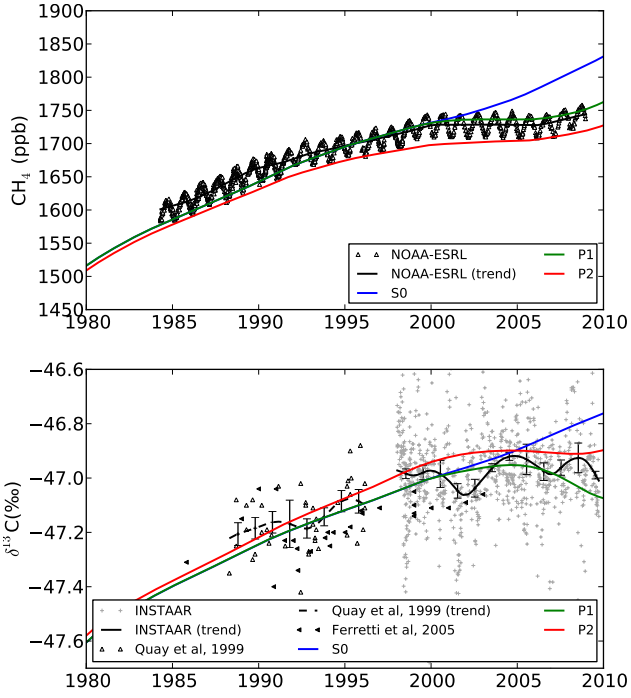

Fig. 4. Comparison of simulated and measured CH_4 and δ^{13}C-CH_4 for the initial scenario S0 and the two proposed scenarios P1 and P2, at the station of Cape-Grim, Australia.

One example is the scenario P1, which is presented in Fig. 4: It assumes a 10 % reduction of wetland emissions between 2002 and 2006. To reduce the δ^{13}C-CH_4 mismatch requires a reduction of biomass burning emissions of 18 % between 2002 and 2008, and a fossil fuel emissions growth-rate as low as 1 % yr^{-1}, which is at the lowest range of the EDGAR4.0 growth-rate confidence interval for the period 2000–2005.

On the other hand, if we assume that an increase in OH explains a major part of the CH_4 growth-rate slowdown as shown in scenario S5, several scenarios involving a decrease in ^{13}C enriched or an increase in ^{13}C depleted sources can explain the observed δ^{13}C-CH_4 trend.

To investigate this option we constructed scenario P2, presented also in Fig. 4. We assumed an increase of OH concentrations by 0.2 % yr^{-1} between 1985 and 2000, and by 0.6 % yr^{-1} after 2000, to compensate for the increased anthropogenic emissions. Similarly to P1, we assumed a 18 % decrease of biomass burning emissions between 2002 and 2008, but instead of reducing the fossil fuel emissions growth-rate, we assumed a 0.5 % yr^{-1} growth-rate of natural wetland emissions between 1990 and 2010.

The results produced by the scenarios P1 and P2 are in much closer agreement with the measurements than the initial scenario, S0. However scenario P1 requires relatively

strong reduction of the fossil fuel increases, which calls for further verification. If the strong increase in fossil fuel emissions from the EDGAR4.0 inventory is confirmed, then the only option is an increase in OH.

Scenarios P1 and P2 should be regarded as extreme options, spanning the range of a negligible to a large influence of OH. It is possible to explain the stabilization of the methane concentrations by a combination of a smaller increase in OH and a smaller reduction of wetland emissions than in P1 and P2.

4 Conclusions

Model simulations of CH_4 and δ^{13}C-CH_4 over the last 40 yr were carried out to test different scenarios against the available measurements. In our base scenario, anthropogenic emissions were specified according to the EDGAR4.0 emission inventory, and natural sources as well as the methane lifetime were assumed to be the same each year. This scenario leads to increasing methane concentrations and δ^{13}C-CH_4 throughout the simulation, whereas the measurements show stabilization of these parameters after 2000. The size of the adjustments needed to bring the model in agreement with the measurements exceeds the uncertainty range of the anthropogenic emissions estimates and therefore the observed trends can only be explained by a reduction of natural sources, and/or a change in methane lifetime compensating the anthropogenic increase.

Two classes of scenarios were built to evaluate these hypotheses: (1) scenarios assuming a constant methane lifetime, (2) scenarios that assume increasing OH concentrations and a corresponding reduction in the methane lifetime, within the uncertainty of MCF analysis. Both classes require a shift towards an isotopically lighter source mixture. In addition, the first class requires a decrease of natural emissions of 20 Tg CH_4 yr^{-1} in average on the period 2000–2010. Given the size of this emission decrease it is most likely explained by a reduction of wetland emissions after 2000. As this reduction further enriches the source mixture in ^{13}C, significant reductions of isotopically heavy sources (such as biomass burning and fossil fuel emissions) are needed to explain the δ^{13}C-CH_4 measurements. In the second class of scenarios most of the methane growth-rate slowdown is explained by increasing OH concentrations. This induces a smaller ^{13}C enrichment of the atmosphere than the reduction of wetlands emissions required under class 1, which can be further compensated by a limited and therefore more plausible additional adjustments to the source fuel mixture. Independently of the chosen OH scenario, a reduction in biomass burning and/or of the growth-rate of fossil fuel emissions is needed to explain the δ^{13}C-CH_4 measurements. However, assuming a positive trend in OH brings the required emission adjustments into a more realistic regime.

δD-CH_4 could provide further confirmation of the possible role of increasing OH concentrations. However, the limited availability of measurements and the high uncertainty of the isotopic ratios of sources so far prevented us from deriving any significant additional constraints. At this stage, we can only recommend that future studies consider the possibility of changing OH concentrations.

This study demonstrates the value of isotopic measurements for studying the global CH_4 trend. An important limitation that we encountered is the limited continuity of isotopic measurements for our period of study. Therefore we plead for continuation of high quality time-series for δ^{13}C-CH_4. An improved availability of δD-CH_4 measurements could provide important additional constraints, but would require an improved isotopic characterization of source process.

Acknowledgements. We would like to acknowledge Michiel van Weele (KNMI) and Maarten Krol (WUR/IMAU) for their useful discussions on the potential role of OH. This project was funded by the Dutch NWO under grant number 865.07.007.

Edited by: M. Heimann

References

Allan, W., Manning, M. R., Lassey, K. R., Lowe, D. C., and Gomez, A. J.: Modeling the variation of δ^{13}C in atmospheric, Global Biogeochem. Cy., 15, 467–481, 2001.

Allan, W., Lowe, D. C., Gomez, A. J., Struthers, H., and Brailsford, G. W.: Interannual variation of ^{13}C in tropospheric methane: Implications for a possible atomic chlorine sink in the marine boundary layer, J. Geophys. Res., 110, D11306, doi:10.1029/2004JD005650, 2005.

Allan, W., Struthers, H., and Lowe, D. C.: Methane carbon isotope effects caused by atomic chlorine in the marine boundary layer: Global model results compared with Southern Hemisphere measurements, J. Geophys. Res., 112, D04306, doi:10.1029/2006JD007369, 2007.

Bergamaschi, P., Braünlich, M., Marik, T., and Brenninkmeijer, C. A. M.: Measurements of the carbon and hydrogen isotopes of atmospheric methane at Izaña, Tenerife: Seasonal cycles and synoptic-scale variations, J. Geophys. Res., 105, 14531–14546, doi:doi:10.1029/1999JD901176, 2000.

Bousquet, P., Ciais, P., Miller, J. B., Dlugokencky, E. J., Hauglustaine, D. A., Prigent, C., Van Der Werf, G. R., Peylin, P., Brunke, E.-G., Carouge, C., Langenfelds, R. L., Lathière, J., Papa, F., Ramonet, M., Schmidt, M., Steele, L. P., Tyler, S. C., and White, J.: Contribution of anthropogenic and natural sources to atmospheric methane variability, Nature, 443, 439–443, doi:10.1038/nature05132, 2006.

Braünlich, M., Aballain, O., Marik, T., Jöckel, P., Brenninkmeijer, C. A. M., Chappelaz, J., Barnola, J.-m., Mulvaney, R., and Sturges, W.: Changes in the global atmospheric methane budget over the last decades inferred from δ^{13}C and D isotopic analysis of Antarctic firn air, J. Geophys. Res., 106, 20465–20481, 2001.

de Laeter, J. R., Böhlke, J. K., De Bièvre, P., Hidaka, H., Peiser, H. S., Rosman, K. J. R., and Taylor, P. D. P.: Atomic weights

of the elements. Review 2000 (IUPAC Technical Report), Pure Appl. Chem., 75, 683–799, doi:10.1351/pac200375060683, 2003.

Denman, K., G, B., Chidthaisong, A., Ciais, P., Cox, P. M., Dickinson, R. E., Hauglustaine, D., Heinze, C., Holland, E., Jacob, D., Lohmann, U., Ramachandran, S., da Silva Dias, P. L., Wofsy, S. C., and Zhang, X.: Couplings Between Changes in the Climate System and Biogeochemistry, Cambridge University Press, Cambridge, UK and NY, NY, USA, 499–587, 2007.

Dentener, F., van Weele, M., Krol, M., Houweling, S., and van Velthoven, P.: Trends and inter-annual variability of methane emissions derived from 1979–1993 global CTM simulations, Atmos. Chem. Phys., 3, 73–88, doi:10.5194/acp-3-73-2003, 2003.

Dlugokencky, E. J., Lang, P. M., and Masarie, K. A.: Atmospheric Methane Dry Air Mole Fractions from the NOAA ESRL Carbon Cycle Cooperative Global Air Sampling Network, available online at: ftp://ftp.cmdl.noaa.gov/ccg/, 2010.

Dlugokencky, E. J., Masarie, K. A., Lang, P. M., and Tans, P. P.: Continuing decline in the growth rate of the atmospheric methane burden, Nature, 393, 447–450, 1998.

Dlugokencky, E. J., Houweling, S., Bruhwiler, L., Masarie, K. A., Lang, P. M., Miller, J. B., and Tans, P. P.: Atmospheric methane levels off: Temporary pause or a new steady-state?, Geophys. Res. Lett., 30, ASC5, doi:10.1029/2003GL018126, 2003.

Dlugokencky, E. J., Bruhwiler, L., White, J. W. C., Emmons, L. K., Novelli, P. C., Montzka, S. A., Masarie, K. A., Lang, P. M., Crotwell, A. M., Miller, J. B., and Gatti, L. V.: Observational constraints on recent increases in the atmospheric CH_4 burden, Geophys. Res. Lett., 36, L18803, doi:10.1029/2009GL039780, 2009.

Etheridge, D. M., Steele, L. P., Francey, R. J., and Langenfelds, R. L.: Atmospheric methane between 1000 A.D. and present : Evidence of anthropogenic emissions and climatic variability, J. Geophys. Res., 103, 15979–15993, 1998.

Etiope, G. and Milkov, A. V.: A new estimate of global methane flux from onshore and shallow submarine mud volcanoes to the atmosphere, Environmental Geology, 46, 997–1002, doi:10.1007/s00254-004-1085-1, 2004.

Etiope, G., Martinelli, G., Caracausi, A., and Italiano, F.: Methane seeps and mud volcanoes in Italy: Gas origin, fractionation and emission to the atmosphere, Geophys. Res. Lett., 34, L14303, doi:10.1029/2007GL030341, 2007.

Etiope, G., Lassey, K. R., Klusman, R. W., and Boschi, E.: Reappraisal of the fossil methane budget and related emission from geologic sources, Geophys. Res. Lett., 35, 1–5, doi:10.1029/2008GL033623, 2008.

Ferretti, D. F., Miller, J. B., White, J. W. C., Etheridge, D. M., Lassey, K. R., Lowe, D. C., MacFarling Meure, C. M., Dreier, M. F., Trudinger, C. M., van Ommen, T. D., and Langenfelds, R. L.: Unexpected Changes to the Global Methane Budget over the past 2000 years, Science, 309, 1714–1717, doi:10.1126/science.1115193, 2005.

Fiore, A. M., Horowitz, L. W., Dlugokencky, E. J., and West, J. J.: Impact of meteorology and emissions on methane trends, 1990–2004, Geophys. Res. Lett., 33, 1–4, doi:10.1029/2006GL026199, 2006.

Francey, R. J., Manning, M. R., Allison, C. E., Coram, S. A., Etheridge, D. M., Langenfelds, R. L., Lowe, D. C., and Steele, L. P.: A history of $\delta^{13}C$ in atmospheric CH_4 from the Cape Grim Air Archive and Antarctic firn air, J. Geophys. Res., 104, 23631–23643, 1999.

Heimann, M. and Körner, S.: The Global Atmospheric Tracer Model TM3, Max Planck Institut für Biogeochemie, 2003.

Hein, R., Crutzen, P. J., and Heimann, M.: An inverse modeling approach to investigate the global atmospheric methane cycle, Glob. Biogeochem. Cy., 11, 43–76, 1997.

Houweling, S., Kaminski, T., Dentener, F., Lelieveld, J., and Heimann, M.: inverse modeling of methane sources and sinks using the adjoint of a global transport model, J. Geophys. Res., 104, 26137–26160, 1999.

Houweling, S., Dentener, F., Lelieveld, J., Walter, B., and Dlugokencky, E. J.: The modeling of tropospheric methane: How well can point measurements be reproduced by a global model?, J. Geophys. Res., 105, 8981–9002, 2000.

Houweling, S., Röckmann, T., Aben, I., Keppler, F., Krol, M., Meirink, J. F., Dlugokencky, E. J., and Frankenberg, C.: Atmospheric constraints on global emissions of methane from plants, Geophys. Res. Lett., 33, doi:10.1029/2006GL026162, 2006.

Jones, D. B. A., Andrews, A. E., Schneider, H. R., and McElroy, M. B.: Constraints on meridional transport in the stratosphere imposed by the mean age of air in the lower stratosphere, J. Geophys. Res., 106, 10243–10256, doi:10.1029/2000JD900745, 2001.

Judd, A. G., Hovland, M., Dimitrov, L. I., García Gil, S., and Jukes, V.: The geological methane budget at Continental Margins and its influence on climate change, Geofluids, 2, 109–126, doi:10.1046/j.1468-8123.2002.00027.x, 2002.

Kalnay, E., Kanamitsu, M., Kistler, R., Collins, W., Deaven, D., Gandin, L., Iredell, M., Saha, S., White, G., Woollen, J., Zhu, Y., Chelliah, M., Ebisuzaki, W., Higgins, W., Janowiak, J., Mo, K. C., Ropelewski, C., Wang, J., Leetmaa, A., Reynolds, R., Jenne, R., and Joseph, D.: The NCEP/NCAR 40-Year Reanalysis Project, bulletin of the american meteorologist society, 77, 437–471, 1996.

Karlsdóttir, S. and Isaksen, I. S. A.: Changing methane lifetime: Possible cause for reduced growth, Geophys. Res. Lett., 27, 93–96, 2000.

Krol, M. and Lelieveld, J.: Can the variability in tropospheric OH be deduced from measurements of 1,1,1-trichloroethane (methyl chloroform)?, J. Geophys. Res., 108, ACH16, doi:10.1029/2002JD002423, 2003.

Lassey, K. R., Lowe, D. C., and Manning, M. R.: The trend in atmospheric methane $\delta^{13}C$ and implications for isotopic constraints on the global methane budget, Glob. Biogeochem. Cy., 14, 41–49, 2000.

Lassey, K. R., Etheridge, D. M., Lowe, D. C., Smith, A. M., and Ferretti, D. F.: Centennial evolution of the atmospheric methane budget: what do the carbon isotopes tell us?, Atmos. Chem. Phys., 7, 2119–2139, doi:10.5194/acp-7-2119-2007, 2007.

Lassey, K. R., Brailsford, G. W., Bromley, A. M., Martin, R. J., Moss, R. C., Gomez, A. J., Sherlock, V., Allan, W., Nichol, S. E., Schaefer, H., Connor, B. J., Robinson, J., and Smale, D.: Recent changes in methane mixing ratio and its ^{13}C content observed in the southwest Pacific region, J. Int. Environ. Sci., 7, 109–117, doi:10.1080/19438151003621441, 2010.

Law, K. S. and Pyle, J. A.: Modeling Trace Gas Budgets in the Troposphere 2. CH_4 and CO, J. Geophys. Res., 98, 18401–18412, doi:10.1029/93JD01480, 1993.

Lelieveld, J., Peters, W., Dentener, F. J., and Krol, M. C.: Stability of tropospheric hydroxyl chemistry, J. Geophys. Res., 107, ACH17, doi:10.1029/2002JD002272, 2002.

Louis, J.-F.: A parametric model of vertical eddy fluxes in the atmosphere, Boundary Layer Meteorology, 17, 187–202, 1979.

MacFarling Meure, C., Etheridge, D., Trudinger, C., Steele, P., Langenfelds, R., van Ommen, T., Smith, A., and Elkins, J.: Law Dome CO_2 , CH_4 and N_2O ice core records extended to 2000 years BP, Geophys. Res. Lett., 33, L14810, doi:10.1029/2006GL026152, 2006.

Mikaloff Fletcher, S. E., Tans, P. P., Bruhwiler, L. M., Miller, J. B., and Heimann, M.: CH_4 sources estimated from atmospheric observations of CH_4 and its $^{13}C/^{12}C$ isotopic ratios: 1. Inverse modeling of source processes, Glob. Biogeochem. Cy., 18, GB4004, doi:10.1029/2004GB002223, 2004a.

Mikaloff Fletcher, S. E., Tans, P. P., Bruhwiler, L. M., Miller, J. B., and Heimann, M.: CH_4 sources estimated from atmospheric observations of CH_4 and its $^{13}C/^{12}C$ isotopic ratios: 2. Inverse modeling of CH 4 fluxes from geographical regions, Glob. Biogeochem. Cy., 18, GB4005, doi:10.1029/2004GB002224, 2004b.

Miller, J. B., Mack, K. A., Dissly, R., White, James, W. C., Dlugokencky, E. J., and Tans, P. P.: Development of analytical methods and measurements of $^{13}C/^{12}C$ in atmospheric CH_4 from the NOAA Climate Monitoring and Diagnostics Laboratory Global Air Sampling Network, J. Geophys. Res., 107, ACH11, doi:10.1029/2001JD000630, 2002.

Mischler, J. A., Sowers, T. A., Alley, R. B., Battle, M., McConnell, J. R., Mitchell, L., Popp, T., Sofen, E., and Spencer, M. K.: Carbon and hydrogen isotopic composition of methane over the last 1000 years, Glob. Biogeochem. Cy., 23, GB4024, doi:10.1029/2009GB003460, 2009.

Neef, L., van Weele, M., and van Velthoven, P.: Optimal estimation of the present-day global methane budget, Global Biogeochem. Cy., 24, GB4024, doi:10.1029/2009GB003661, http://www.agu.org/pubs/crossref/2010/2009GB003661.shtml, 2010.

Prinn, R., Cunnold, D., Simmonds, P., Alyea, F., Boldi, R., Crawford, A., Fraser, P., Gutzler, D., Hartley, D., Rosen, R., and Rasmussen, R.: Global Average Concentration and Trend for Hydroxyl Radicals Deduced from ALA/GAGE Trichloroethane (Metgyl Chloroform) Data for 1978-1990, J. Geophys. Res., 97, 2445–2461, 1992.

Prinn, R. G., Huang, J., Weiss, R. F., Cunnold, D. M., Fraser, P. J., Simmonds, P. G., McCulloch, A., Harth, C., Reimann, S., Salameh, P., O'Doherty, S., Wang, R. H. J., Porter, L. W., Miller, B. R., and Krummel, P. B.: Evidence for variability of atmospheric hydroxyl radicals over the past quarter century, Geophys. Res. Lett., 32, doi:10.1029/2004GL022228, 2005.

Quay, P., Stutsman, J., Wilbur, D., Snover, A., Dlugokencky, E. J., and Brown, T.: The isotopic composition of atmospheric methane, Glob. Biogeochem. Cy., 13, 445–461, 1999.

Quay, P. D., King, S. L., Lansdown, J. M., and Wilbur, D. O.: Isotopic composition of methane released from wetlands: implications for the increase in atmospheric methane, Global Biogeochem. Cy., 2, 385–397, 1988.

Randerson, J. T., van Der Werf, G. R., Giglio, L., Collatz, G. J., and Kasibhatla, P. S.: Global Fire Emissions Database version 2.1 (GFEDv2.1), 2007.

Rigby, M., Prinn, R. G., Fraser, P. J., Simmonds, P. G., Langenfelds, R. L., Huang, J., Cunnold, D. M., Steele, L. P., Krummel, P. B., Weiss, R. F., O'Doherty, S., Salameh, P. K., Wang, H. J., Harth, C. M., Mühle, J., and Porter, L. W.: Renewed growth of atmospheric methane, Geophysical Research Letters, 35, L22805, doi:10.1029/2008GL036037, http://www.agu.org/pubs/crossref/2008/2008GL036037.shtml, 2008.

Russel, G. L. and Lerner, J. A.: A new finite-differencing scheme for the tracer transport equation, J. Appl. Meteorol., 20, 1483–1498, 1981.

Sander, S. P., Friedl, R. R., Golden, D. M., Kurylo, M. J., Moortgat, G. K., Wine, P. H., Ravishankara, A. R., Kolb, C. E., Molina, M. J., Finlayson-Pitts, B. J., Huie, R. E., and Orkin, V. L.: Chemical Kinetics and Photochemical Data for Use in Atmospheric Studies Evaluation Number 15, JPL Publication 06-2, 2006.

Sanderson, M. G.: Biomass of termites and their emissions of methane and carbon dioxide: a global database, Glob. Biogeochem. Res., 10, 543–557, 1996.

Scheele, E. A., Irving, W. N., and Krugre, D.: Global anthropogenic methane emissions, Rotterdam, millpress edn., 257–262, 2002.

Tans, P. P.: A note on isotopic ratios and the global atmospheric methane budget, Glob. Biogeochem. Cy., 11, 77–81, doi:10.1029/2002GB001895, 1997.

Tiedtke, M.: A comprehensive mass flux scheme for cumulus parametrization in large-scale models, Mon. Weather Rev., 117, 1779–1800, 1989.

Tyler, S. C., Rice, A. L., and Ajie, H. O.: Stable isotope ratios in atmospheric CH_4 : Implications for seasonal sources and sinks, J. Geophys. Res., 112, D03303, doi:10.1029/2006JD007231, 2007.

Velders, G.: Description of the RIVM 2-dimensional stratosphere model, RIVM Report 722201002, 1995.

Walter, B. P., Heimann, M., and Matthews, E.: Modeling modern methane emissions from natural wetlands 2. Interannual variations 19821993, J. Geophys. Res., 106, 34207–34219, doi:10.1029/2001JD900164, 2001.

Wang, J. S., Logan, J. A., Mcelroy, M. B., Duncan, B. N., Megretskaia, I. A., and Yantosca, R. M.: A 3-D model analysis of the slowdown and interannual variability in the methane growth rate from 1988 to 1997, Glob. Biogeochem. Cy., 18, GB3011, doi:10.1029/2003GB002180, 2004.

Wania, R., Ross, I., and Prentice, I. C.: Implementation and evaluation of a new methane model within a dynamic global vegetation model: LPJ-WHyMe v1.3.1, Geosci. Model Dev., 3, 565–584, doi:10.5194/gmd-3-565-2010, 2010.

Wuebbles, D. J. and Hayhoe, K.: Atmospheric methane and global change, Earth-Sci. Rev., 57, 177 – 210, 2002.

Yamada, K., Ozaki, Y., Nakagawa, F., Sudo, S., Tsuruta, H., and Yoshida, N.: Hydrogen and carbon isotopic measurements of methane from agricultural combustion: Implications for isotopic signatures of global biomass burning sources, J. Geophys. Res., 111, D16306, doi:10.1029/2005JD006750, 2006.